International Journal on Magnetic Particle Imaging
Vol 8, No 1, Suppl 1, Article ID 2203033, 3 Pages

Infinite Science Publishing

Proceedings Article

1D Imaging with a Single-Sided FFL Magnetic Particle Imaging Scanner

Chris McDonough [a] · Alexey Tonyushkin [a,*]

[a] Physics Department, Oakland University, Rochester, MI 48309 USA
[*] Corresponding author, email: tonyushkin@oakland.edu

Abstract

Over the past decade, various MPI scanner topologies have been demonstrated, which include a single-sided scanner. Such a scanner features all its hardware located on one side, offering accessibility without limitations due to the size of the object of interest. The original scanner design utilized a field-free point making it very robust in the hardware implementation. In our design of a single-sided scanner we utilize a field-free line, which provides higher sensitivity and robust image reconstruction. In this work we demonstrate first one-dimensional imaging with a single-sided field-free line MPI scanner.

I. Introduction

Recent developments in MPI include scanners with head-size bore that can potentially accommodate humans [1, 2]. Our single-sided field-free line (FFL) scanner may allow imaging of body regions of a large subject including human. The very first implementation of a single-sided geometry with field-free point (FFP) was demonstrated in [3] and the multidimensional imaging was presented in [4–6]. In our device, the excitation and selection fields are generated by an elongated drive coil and a pair of co-planar elongated coils, respectively as described in [7, 8]. However, the typical challenge for imaging associated with the unilateral geometry of the coils is that the magnetic field profiles are inherently inhomogeneous [9] as well as significantly more noisy background then in the confined geometries. In this work, we demonstrate one-dimensional (1D) imaging of specially designed phantoms consisting of multiple rods using our single-sided device. Moreover, such imaging was performed at relatively low field gradients at the height of more than 10 mm above the surface with a spatial resolution of up to 2 mm after the deconvolution with the experimentally obtained point-spread function (PSF).

II. Methods and materials

II.I. Scanner design and Operation

The hardware implementation of our FFL single-sided scanner is described in [8]. Two out of three racetrack coils referred to as selection field (SF) coils create an FFL. By altering the currents in the SF coils the position of the FFL can be shifted thus encoding the trajectory. The third racetrack coil creates an excitation field and is referred to as the drive field (DF) coil. The DF coils also can be used to supply bias field allowing for further control of the FFL trajectory [9]. The excitation waveform at f_0 =25 kHz is produced by an ultra-low distortion function generator DS360 (Stanford Research Systems, Sunnyvale, CA, USA), which is followed by a power amplifier Techron 7548 (AE Techron, Elkhart, IN, USA) and then passed through a custom-made high-power resonant low-pass filter. The signal from tracer is received by a circular receive (Rx) coil in a gradiometer configuration at the surface of the scanner and then passed through a custom-made notch and high-pass filters. The 3^{rd} harmonic, $3f_0$ =75 kHz of the signal is measured in a Lock-In Amplifier SR830 DPS (Stanford Research Systems, Sunnyvale, CA, USA) and the time series of that harmonic is recorded using a LabView (National Instruments, Austin, TX, USA) acquisition interface.

II.II. Phantom design

For 1D imaging, we designed several phantoms using a 3D printer Form3 (Formlabs, Somerville, MA, USA). The phantoms consist of different number of capillaries 20 mm long and 1.2 mm diameter filled with undiluted Synomag-D (Micromod, Rostock, Germany) superparamagnetic nanoparticles (SPIONs). During the imaging the rods are positioned in parallel to the FFL so that the single rod is located along the FFL at the isocenter of the scanner and 17 mm above the scanner's surface and the double rods are located in the plane at the height of 15.5 mm symmetrically with respect to the isocenter with a spacing $d = 20$ mm between them as shown in Fig. 2(b).

II.III. 1D Imaging

In the imaging experiments we use a drive field with a strength of 1.8 mT at the surface of the scanner. Two dc power supplies (Delta Elektronika SM3300, Netherlands) each with a current of 40 A create a magnetic field gradient at a static position 17 mm above the surface with a strength of 0.42 T m^{-1}. The position of the FFL can be shifted in the plane parallel to the surface of the scanner by varying the current in the two power supplies [8]. The trajectory of FFL is programmed by LabView interface to automatically encode the FFL trajectory across the phantom with 2 mm step size within 4 cm field of view (FOV). To mitigate background effects, including eddy currents generated in the system, and obtain a large SNR$\sim$100 the signal was sampled for 2 s at each FFL position. Additionally, to further reduce background effects, a second scan was performed without the phantom to be subtracted from the total signal.

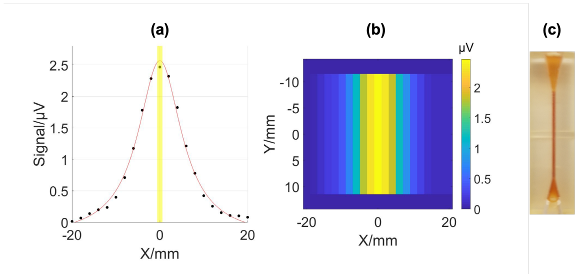

Figure 1: 1D image of central rod phantom at the height of 17 mm: (a) measured projection of central rod phantom (shown by vertical bar) at G =0.32 T m^{-1}, fit to a Lorentzian with a FWHM of 12 mm, (b) rendered pseudo-2D image of the phantom, (c) 3D printed phantom.

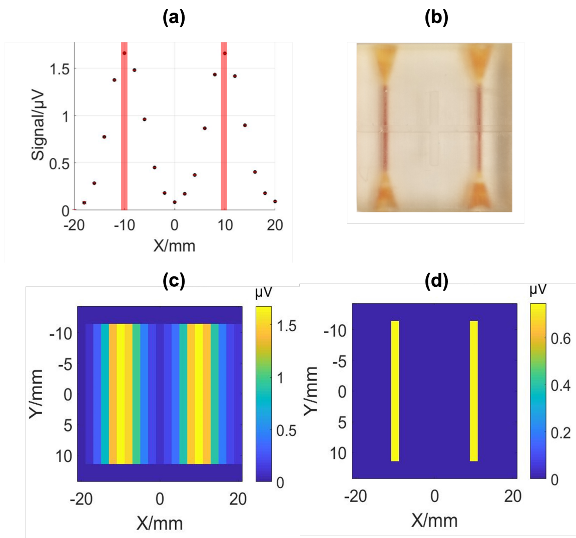

Figure 2: 1D image of double rod phantom at the height of 15.5 mm: (a) the measured projection of the phantom (shown by vertical bars); (b) 3D printed phantom; (c) rendered pseudo-2D image of the phantom; (d) deconvolved pseudo-2D image of the phantom.

III. Results and Discussion

To study imaging performance of our scanner we measured the signal from multiple rod phantoms filled with SPIONs. Such signal in 1D imaging mode relates to a projection imaging made at zero angle. The simplest 1D image is shown in Fig. 1 as obtained from a single rod phantom filled with SPIONs and orientated parallel to the FFL. Due to the system's spatial resolution less than the size of the rod we can treat the corresponding image as a system's PSF (see the example in Fig. 1(a)). We further use the experimentally obtained PSF to perform image deconvolution using the standard Richardson-Lucy deconvolution algorithm [10].

To study the uniformity of the image across maximum FOV and demonstrate spatial resolution we used a double rod phantom. Fig. 2 shows the results of 1D imaging of the 20 mm separation phantom. It can be seen in Fig. 2(a) that the signal is uniform across 4 cm FOV at the operating height of 15.5 mm without distortion and 20 mm separation can be resolved with 100% contrast. In addition, deconvolving the raw data with an experimental PSF, an SPION distribution that perfectly match the phantom can be reconstructed with up to 2 mm resolution as limited by the encoding step (see Fig. 2(d)).

IV. Conclusion

We presented first experimental results on 1D imaging with a single-sided FFL MPI scanner. The results show uniform images of rod phantoms located at the height of 17 mm and 15.5 mm above the surface across 4 cm FOV.

10.18416/ijmpi.2022.2203033

By deconvolving the image with the experimental PSF an accurate reconstruction of the phantom image with up to 2 mm resolution can be obtained. In the future we will extend imaging to 2D by implementing rotation of the subject.

Acknowledgments

Research funding: this work is supported by NIH under Award R15EB028535.

Author's statement

Conflict of interest: Authors state no conflict of interest.

References

[1] J. Rahmer, A. Halkola, B. Gleich, I. Schmale, and J. Borgert. First experimental evidence of the feasibility of multi-color magnetic particle imaging. *Physics in medicine and biology*, 60(5):1775–91, 2015, doi:10.1088/0031-9155/60/5/1775.

[2] M. Graeser, F. Thieben, P. Szwargulski, F. Werner, N. Gdaniec, M. Boberg, F. Griese, M. Möddel, P. Ludewig, D. van de Ven, O. M. Weber, O. Woywode, B. Gleich, and T. Knopp. Human-sized magnetic particle imaging for brain applications. *Nature Communications*, 10(1), 2019, doi:10.1038/s41467-019-09704-x.

[3] T. F. Sattel, T. Knopp, S. Biederer, B. Gleich, J. Weizenecker, J. Borgert, and T. M. Buzug. Single-sided device for magnetic particle imaging. *Journal of Physics D: Applied Physics*, 42(2):022001, 2009, doi:10.1088/0022-3727/42/2/022001.

[4] C. Kaethner, M. Ahlborg, K. Grafe, G. Bringout, T. F. Sattel, and T. M. Buzug. Asymmetric Scanner Design for Interventional Scenarios in Magnetic Particle Imaging. *IEEE Transactions on Magnetics*, 51(2):1–4, 2015, doi:10.1109/TMAG.2014.2337931.

[5] K. Gräfe, A. von Gladiss, G. Bringout, M. Ahlborg, and T. M. Buzug. 2D Images Recorded With a Single-Sided Magnetic Particle Imaging Scanner. *IEEE Transactions on Medical Imaging*, 35(4):1056–1065, 2016, doi:10.1109/TMI.2015.2507187.

[6] A. von Gladiss, Y. Blancke Soares, T. M. Buzug, and K. Gräfe, Dynamic imaging with a 3d single-sided mpi scanner, in *International Workshop on Magnetic Particle Imaging*, 235–236, 2019.

[7] A. Tonyushkin. Single-Sided Field-Free Line Generator Magnet for Multi-Dimensional Magnetic Particle Imaging. *IEEE Transactions on Magnetics*, 53(9):5300506, 2017, doi:10.1109/TMAG.2017.2718485.

[8] J. Pagan, C. McDonough, T. Vo, and A. Tonyushkin. Single-sided magnetic particle imaging device with field-free-line geometry for in vivo imaging applications. *IEEE Transactions on Magnetics*, 57(2):1–5, 2021, doi:10.1109/TMAG.2020.3008596.

[9] C. Chinchilla, C. McDonough, A. Negash, J. Pagan, and A. Tonyushkin. Simulation studies of image reconstruction for field free line single-sided magnetic particle imaging scanner. *International journal on magnetic particle imaging*, 7(1):2104001, 2021.

[10] T. Bose, F. Meyer, and M. Chen, Digital Signal and Image Processing. Wiley, 2004, ISBN: 9780471452300. URL: https://books.google.com/books?id=F%5C_NyQgAACAAJ.

